Volume 1 | Number 1 | Jan 2013 | Pages 1–100

ChemComm

Chemical Communications
www.rsc.org/chemcomm

ROYAL SOCIETY OF CHEMISTRY

This is an *Accepted Manuscript*, which has been through the Royal Society of Chemistry peer review process and has been accepted for publication.

Accepted Manuscripts are published online shortly after acceptance, before technical editing, formatting and proof reading. Using this free service, authors can make their results available to the community, in citable form, before we publish the edited article. We will replace this *Accepted Manuscript* with the edited and formatted *Advance Article* as soon as it is available.

You can find more information about *Accepted Manuscripts* in the **Information for Authors**.

Please note that technical editing may introduce minor changes to the text and/or graphics, which may alter content. The journal's standard **Terms & Conditions** and the **Ethical guidelines** still apply. In no event shall the Royal Society of Chemistry be held responsible for any errors or omissions in this *Accepted Manuscript* or any consequences arising from the use of any information it contains.

ROYAL SOCIETY OF CHEMISTRY

www.rsc.org/chemcomm

Journal Name

COMMUNICATION

Bimetallic Coordination Polymer as a Promising Anode Material for Lithium-Ion Batteries

Chao Li, Xiaoshi Hu, Xiaobing Lou, Qun Chen and Bingwen Hu[*]

Bimetallic coordination polymers (BiCPs) with Zn and Co elements were synthesized and applied as anode materials. When the rate is increased to 2 A g^{-1}, a capacity of 622 mAh g^{-1} after 500 cycles could still be maintained.

Among room-temperature rechargeable batteries, lithium-ion chemistry is currently unrivalled in terms of energy and power densities.[1-5] The development of high-performance electrode materials is stringent for state-of-the-art lithium-ion batteries (LIBs) and their wide range of applications (e.g., plug-in hybrid electric vehicles, stationary storage, smart grids, etc.).[6-8] Graphite is presently used as the commercial anode material for lithium-ion batteries, however, it has a limited theoretical capacity of around 372 mAh g^{-1} because of the formation of the intercalation compound LiC$_6$. As a consequence, considerable effort has been devoted to developing other high-capacity anode materials. Among those possible alternatives, a lot of work has been devoted to metal oxides,[9-13] Sn-based composites,[14-20] P-based composites,[21] Si-based composites,[22-24] because of their ability to react reversibly with large amounts of Li per formula unit. However, large volume changes generally occur in these host materials during lithium insertion/extraction, which leads to pulverization, particle aggregation, and pile-up of solid-electrolyte interphase (SEI) layers on the surface, thus resulting in rapid capacity fading. Though several kinds of alternatives have been reported, it is still a great challenge to fabricate neotype anode materials with high reversible capacity and excellent structural stability.

Coordination polymers (CPs) or metal-organic frameworks (MOFs) have experienced explosive development as a promising class of microporous or mesoporous materials because of their huge surface area, tunable porosities, and controllable structure.[25-28] A wide range of applications, including gas storage and separation, catalysis, drug delivery, electron and proton

conductivity, benefit from the recent fast development of CPs and MOFs.[29-30] Particularly, pure CPs and MOFs have also been investigated either as cathode or as anode materials. Chen et al. first used MOF (MOF-177) as anode for LIBs.[31] Other MOFs, such as Mn-LCP,[32] Co$_2$(OH)$_2$BDC,[33] Zn$_3$(HCOO)$_6$[34] have also been applied. However, these CPs- or MOFs-based anode materials, with either the limited reversible capacity or the poor rate performance, were not satisfactory for real-world applications. The scaffolding-like nature of MOFs often lead to extraordinarily high apparent surface (>2000 m^2 g^{-1}); however, a very high surface area often leads to increased side reactions with the electrolyte and thus may not be beneficial for LIB performance. MOF-5 has an extremely high surface area (3362 m^2 g^{-1}), however, the MOF-5 structure is water-sensitive and proper water treatment maybe a good way to reduce the apparent surface.

In this communication, to the best of our knowledge, we report a simple method for the synthesis of bimetallic coordination polymer (BiCP) and use it as anode materials for the first time. Our experimental results show that bimetallic system has better electrochemical performance over monometallic system. The bimetallic systems were stimulated by the idea of doping in the cathodes, such as the Al-doping or Zn-doping in the LiCoO$_2$ system. As illustrated in scheme 1, the synthesis protocol only involves a facile hydrothermal reaction to form binary MOF followed by water immersion to produce BiCP, and therefore it is highly promising for mass production. Encouragingly, when applied as anode material, the as-prepared BiCP exhibits an outstanding lithium-storage capacity and impressive rate capability in LIBs. This work might open new possibilities for utilizing CP- or MOF-based electrode materials in LIBs.

Department of Physics, Shanghai Key Laboratory of Magnetic Resonance, Engineering Research Center for Nanophotonics & Advanced Instrument (Ministry of Education), East China Normal University, Shanghai 200062, China. E-mail: bwhu@phy.ecnu.edu.cn
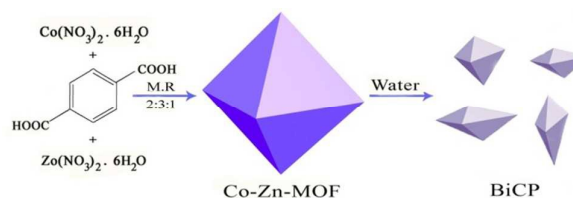
Scheme 1. Schematic illustration for the preparation process of BiCP.

Co[II]-modified MOF-5 synthesized in large quantities through a facile hydrothermal method was used as the starting material. The as-synthesized sample was designated as "Co-Zn-MOF". After water soaking treatment, BiCP was obtained and used for further characterization.

The morphology and microstructure of Co-Zn-MOF and BiCP were investigated by transmission electron microscopy (TEM). Figure 1a shows that Co-Zn-MOF consists of micropillars with diameters of 1.5-2.5 μm and lengths of several micrometers. The smooth surface and uniform contrast throughout the micropillars indicate the absence of the pores inside the micropillars. In addition, the corresponding selected area electron diffraction (SAED) pattern (Figure 1b) shows a set of well-defined spots, indicative of its good crystallinity property. However, after water immersion, a totally different architecture was observed for BiCP. As shown in Figure 1c, the BiCP particles present relative coarse surface and have ruleless pores in their bodies. Moreover, the corresponding SAED pattern shows a nearly amorphous nature of BiCP with little amount of crystallites (Figure 1d). This suggests that this sample is a kind of coordination polymer with amorphous nature, rather than a kind of metal-organic framework with well-defined crystalline structure.
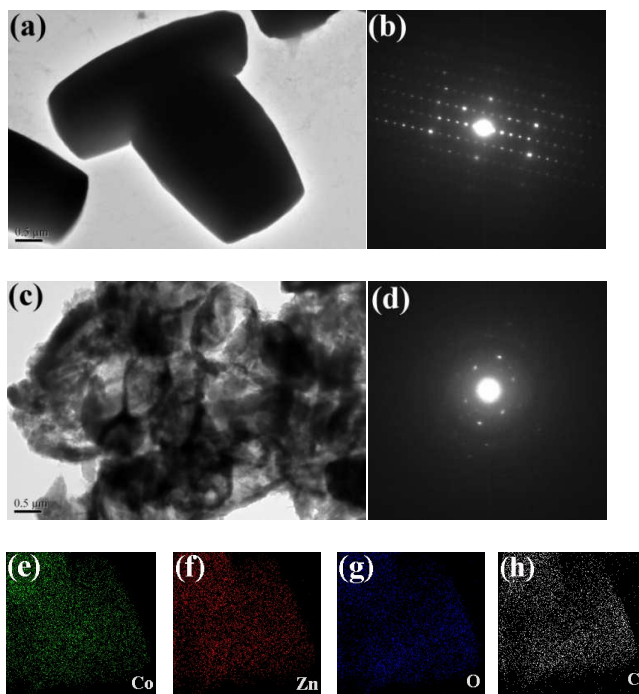
Figure 1. (a) TEM image of Co-Zn-MOF and (b) the corresponding SAED patterns, from which the crystalline nature of Co-Zn-MOF was determined. (c) TEM image of BiCP and (b) the corresponding SAED patterns, from which the amorphous nature of BiCP was determined. (e-h) EDX mapping images of BiCP from selected region.

The Powder X-ray diffraction (PXRD) patterns of Co-Zn-MOF are shown in Figure 2a. The reflection peaks in the Co-Zn-MOF sample are different from pure Co-MOF and Zn-MOF prepared under similar process. The intensive and sharp peaks of Co-Zn-MOF are indicative of a crystalline structure which is consistent with the TEM micropgraphs. After water immersion, all the reflection peaks of

BiCP are different from Co-Zn-MOF (Figure 2b), suggesting the change of the structure. The weak and broad peaks suggested that only a small amount of crystals are existed in the BiCP sample while the majority is in the amorphous form. ^{13}C CP MAS NMR spectra were also carried out for Co-Zn-MOF and BiCP (Figure S1), from which different structures were also determined. Information on the chemical element valence was provided by X-ray photoelectron spectroscopy (XPS). In the high–resolution Co 2p XPS spectrum of BiCP (Figure 2c), two distinct peaks appear at binding energies of 781.53 eV for Co 2p 3/2 and 797.47 eV for Co 2p 1/2, accompanied by two prominent shake-up satellite peaks (785.80 eV and 801.84 eV) beside them, which are characteristic of Co^{2+}. Furthermore, the two distinct peaks appear at binding energies of 1022.39 eV for Zn 2p 3/2 and 1045.35 eV for Zn 2p 1/2 demonstrate the existence of Zn^{2+} (Figure 2d).
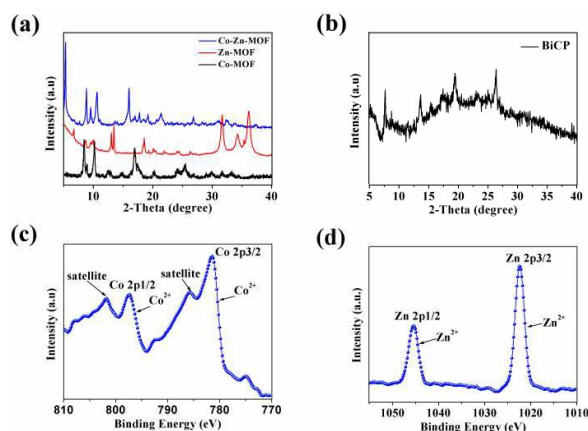
Figure 2. (a) XRD patterns of Co-Zn-MOF, Zn-MOF, Co-MOF and (b) BiCP. (c) High–resolution Co 2p and (d) Zn 2p XPS spectra of BiCP.

The chemical composition of Co-Zn-MOF was analyzed by energy-dispersive X-ray spectroscopy (EDS, Figure S2, Figure S3), where both Co and Zn elements were found to be incorporated within the micropillars. The inductively coupled plasma atomic emission spectroscopy (ICP-AES) results further indicate that the atom ratio of Co/Zn is about 1.52 : 1. Therefore, the formula of Co-Zn-MOF can be expressed as $Co_{0.6}Zn_{0.4}(BDC)(DMF)_x$. It should be mentioned that the Co:Zn molar ratio within Co-Zn-MOF was lower than those of corresponding reactants, which may be due to the fact that Zn^{2+} has a stronger coordination ability than Co^{2+}. A combination of elemental analyses and the PXRD patterns of the as-synthesized samples indicated that the reaction of terephthalic acid ligand with Zn and Co ions could result in bimetallic MOFs as pure phase rather than a mixture of two homometallic MOFs. After water immersion, the atom ratio of Co/Zn in BiCP obtained by ICP-AES turned to be 1.41, and this lower value indicates the collapse of coordinate structure in Co-Zn-MOF, which is consistent with the TEM analysis. Energy dispersive X-ray spectroscopy mapping shown in Figure 1e-h confirmed the coexistence and homogeneous dispersion of Co, Zn, O and C within BiCP particles. The BET surface area of BiCP is about 3.5 $m^2 g^{-1}$, which is obtained from the nitrogen adsorption-desorption isotherms (Figure S4). The low specific surface area of BiCP indicates a small porosity.

To investigate the electrochemical performance of BiCP, two-electrode 2032 coin cells were prepared with BiCP anodes and

lithium metal foil as the counter/reference electrodes. The super-P carbon black is very important to our system due to the low electrical conductivity of MOFs/CPs materials. Figure 3a shows the galvanostatic charge-discharge profiles of the BiCP electrode between 3.0 and 0.01 V vs. Li/Li$^+$ at a rate of 100 mA g^{-1}. The first discharge profile is comprised of three regions located at ca. 1.1, 1.1-0.75 and 0.75-0.01 V (one plateau and two sloping regions, respectively), and most of the specific capacity was delivered at lower than 1 V (ca. 85%). These results are in agreement with the cyclic voltammetry (CV) curves shown in Figure S5. The initial discharge and charge capacities were found to be 2,289 and 1,467 mAh g^{-1}, respectively. All the specific capacities were calculated based on the weight of BiCP. The low Coulombic efficiency of 64.08% of first charge/discharge may be caused by the irreversible capacity loss, including the decomposition of electrolyte to form SEI layers and interfacial lithium storage.[35-38]

The cycling performance of the as-prepared BiCP particles was evaluated at 100 mA g^{-1} over a range of 0.01-3.0V versus Li/Li$^+$. As shown in Figure 3b, the particles show excellent cyclic stability with a high capacity. After 100 cycles, the electrode still maintained a charge capacity of 1,211 mAh g^{-1}, which is approximately 94.98% of the second cycle (1,275 mAh g^{-1}). The reversible capacity of BiCP was largely improved compared with Co-Zn-MOF (710 mAh g^{-1} at 100 cycle), as can be seen in Figure S6. Moreover, such a high reversible capacity of BiCP is even higher than the theoretical capacity of ZnCo$_2$O$_4$ (975.2 mAh g^{-1}), which is a famous Zn, Co-based mixed transition-metal oxide (MTMO) anode material for its good performance and environmental-friendly. This result suggests the potential of BiCP to replace ZnCo$_2$O$_4$ as a future anode material in LIBs. To the best of our knowledge, such an exceedingly high Li storage capacity has not been reported previously for the anode materials from CPs or MOFs. Coulombic efficiency (CE) is another important concern for LIBs.[24,39] For our electrode, the average CE for cycles from the 2nd to 100th is 99.16%, and the nearly 100% CE suggests the stability of the SEI layer and minimal side reactions. However, Our CE was still lower than the requirement for commercial LIBs (>99.994% for 5,000 cycles in a full cell), but can probably be further improved by surface treatments and electrolyte modifications.[40-41]

To understand the electrochemical performance of the as-prepared BiCP particles, we further studied the rate performance of an electrode. Figure 3c presents the rate capabilities and the cycle performance of a BiCP electrode at various current densities (from 100 to 4,000 mA g^{-1}). When the current density gradually increased from 100 to 200, 400, 1,000, 2,000 and 4,000 mA g^{-1}, the corresponding charge capacities at these rates were measured to be 1,200 ± 20, 1,045 ± 8, 880 ± 20, 660 ± 15, 530 ± 10 and 402 ± 2 mAh g^{-1}, respectively; even at 4 A g^{-1}, the reversible capacity is still greater than the theoretical capacity of graphite (372 mAh g^{-1}). After enduring various charge–discharge rates, the BiCP anode swiftly resumes its capacity of about 1,226 mAh g^{-1} with the rate back to 100 mA g^{-1} and the CE is nearly 100%. The slight increase of the charge capacity may also attribute to the reversible growth of a polymeric gel-like layer, which is consistent with the cycling performance test results.[38,42] This result demonstrates that the BiCP particles have a great potential as a high-rate anode material for LIBs. It should be pointed out here that high IR drop ΔU could be observed for higher rates as shown in Figure S7a which is due to relatively high Equivalent Series Resistance (ESR, Figure S7b).
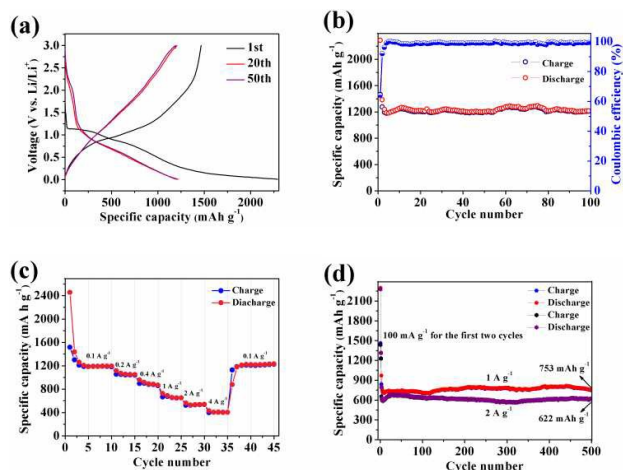
Figure 3. (a) Galvanostatic charge-discharge profiles and (b) Cycle performance of BiCP at a current rate of 100 mA g^{-1}. (c) Rate capability and of amorphous BiCP. (d) Cycling performance of BiCP at high current density (1 A g^{-1} and 2 A g^{-1}). To activate the electrode, a current density of 100 mA g^{-1} was used for the first two cycles, and then the cycling performance of BiCP was evaluated at 1 A g^{-1} and 2 A g^{-1} in the range of 0.01-3.0 V versus Li/Li$^+$. Charge and discharge capacity curves are almost overlapping.

High-rate discharge and charging processes are important for many practical applications of LIBs, including their use in electric vehicles (EVs), hybrid electric vehicles (HEVs) and personal electronics. In general, larger current densities can destroy the structure of electrode materials and result in a rapid capacity loss.[43] However, as shown in Figure 3d, the electrode prepared from BiCP maintained a charge capacity of 753 mAh g^{-1} at 1 A g^{-1} and 622 mAh g^{-1} at 2 A g^{-1} after 500 cycles while maintaining a nearly 100% CE. As a comparison, Co-Zn-MOF showed a quick decrease of charge capacity to less than 450 mAh g^{-1} at a current density of 500 mA g^{-1} after 100 cycles (Figure 4). Such a rapid charging/discharging rate of BiCP could be appealing in many real-world applications.

In summary, bimetallic coordination polymers (BiCPs) were synthesized by a simple method for the first time. Impressively, when applied as anode materials in LIBs, the as-prepared BiCP exhibit ultra-high capacity and impressive rate capability. At a rate of 100 mA g^{-1}, a reversible capacity as high as 1,211 mAh g^{-1} is obtained, and even when the rate is increased to 2 A g^{-1}, a capacity of 622 mAh g-1 could still be maintained. The investigation of the origins of the ultra-high capacity and the lithium-ion motion in this amorphous sample is in progress. We believe that this work will open new possibilities for utilizing CP- or MOF-based electrode materials in LIBs.
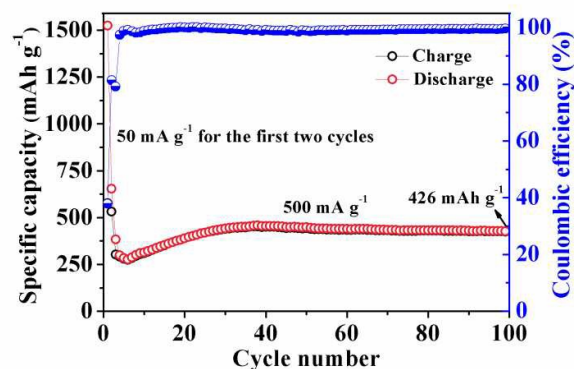
Figure 4. Cycle performance of Co-Zn-MOF at a current rate of 500 mA g^{-1} in the voltage window of 0.01V-3.0V vs Li/Li$^+$.

Notes and references

1. M. Armand, J. M. Tarascon, *Nature*, 2008, **451**, 652-657.
2. J. B. Goodenough, Y. Kim, *Chem. Mater.*, 2010, **22**, 587-603.
3. J. Tarascon, *Nat. chem.*, 2010, **2**, 510.
4. N. Nitta, F. Wu, J. T. Lee, G. Yushin, *Mater. Today*, 2015, **18**, 252-264.
5. D. Larcher, J. Tarascon, *Nat. Chem.*, 2014, **7**, 19-29.
6. J. Cabana, L. Monconduit, D. Larcher, M. R. Palacín, *Adv. Mater.*, 2010, **22**, E170-E192.
7. F. Cheng, J. Liang, Z. Tao, J. Chen, *Adv. Mater.*, 2011, **23**, 1695-1715.
8. W. Xu, J. Wang, F. Ding, X. Chen, E. Nasybulin, Y. Zhang, J.-G. Zhang, *Energy. Environ. Sci.*, 2014, **7**, 513-537.
9. X. Wang, X. Wu, Y. Guo, Y. Zhong, X. Cao, Y. Ma, J. Yao, *Adv. Funct. Mater.*, 2010, **20**, 1680-1686.
10. D. Ge, H. Geng, J. Wang, J. Zheng, Y. Pan, X. Cao, H. Gu, *Nanoscale*, 2014, **6**, 9689.
11. B. Liu, J. Zhang, X. Wang, G. Chen, D. Chen, C. Zhou, G. Shen, *Nano Lett.,* 2012, **12**, 3005-3011.
12. G. Gao, H. B. Wu, B. Dong, S. Ding, X. W. D. Lou, *Adv. Sci.*, 2015, **2**, 1400014.
13. L. Zhou, D. Zhao, X. W. Lou, *Adv. Mater.*, 2012, **24**, 745-748.
14. A. M. Tripathi, S. Mitra, *RSC Adv.*, 2014, **4**, 10358.
15. S. Liu, X. Lu, J. Xie, G. Cao, T. Zhu, X. Zhao, *ACS Appl. Mater. Interfaces*, 2013, **5**, 1588-1595.
16. P. V. Prikhodchenko, D. Y. W. Yu,; S. K. Batabyal, V. Uvarov, J. Gun, S. Sladkevich, A. A. Mikhaylov, A. G. Medvedev, O. Lev, *J. Mater. Chem. A*, 2014, **2**, 8431.
17. P. Chen, Y. Su, H. Liu, Y. Wang, *ACS Appl. Mater. Interfaces*, 2013, **5**, 12073-12082.
18. C. R. Patra, A. Odani, V. G. Pol, D. Aurbach, A. Gedanken, *J. Solid State Electrochem.*, 2006, **11**, 186-194.
19. G. Derrien, J. Hassoun, S. Panero, B. Scrosati, *Adv. Mater.*, 2007, **19**, 2336-2340.
20. W. Zhang, J. Hu, Y. Guo, S. Zheng, L. Zhong, W. Song, L. Wan, *Adv. Mater.*, 2008, **20**, 1160-1165.
21. L. Wang, X. He, J. Li, W. Sun, J. Gao, J. Guo, C. Jiang, *Angew. Chem. Int. Ed.*, 2012, **51**, 9034-9037.
22. X. Li, M. Gu, S. Hu, R. Kennard, P. Yan, X. Chen, C. Wang, M. J. Sailor, J. Zhang, J. Liu, *Nat. Commun.*, 2014, **5**, 4105.
23. N. Liu, Z. Lu, J. Zhao, M. T. McDowell, H. Lee, W. Zhao, Y. Cui, *Nat. Nanotech.*, 2014, **9**, 187-192.
24. H. Wu, G. Chan, J. W. Choi, I. Ryu, Y. Yao, M. T. McDowell, S. W. Lee, A. Jackson, Y. Yang, L. Hu, Y. Cui, *Nat. Nanotech.*, 2012, **7**, 310-315.
25. J. L. C. Rowsell, O. M. Yaghi, *Microporous Mesoporous Mater.*, 2004, **73**, 3-14.
26. A. Shigematsu, T. Yamada, H. Kitagawa, *J. Am. Chem. Soc.*, 2011, **133**, 2034-2036.
27. M. Sadakiyo, H. Ōkawa, A. Shigematsu, M. Ohba, T. Yamada, H. Kitagawa, *J. Am. Chem. Soc.*, 2012, **134**, 5472-5475.
28. S. Bureekaew, S. Horike, M. Higuchi, M. Mizuno, T. Kawamura, D. Tanaka, N. Yanai, S. Kitagawa, *Nat. Mater.*, 2009, **8**, 831-836.
29. A. Morozan, F. Jaouen, *Energy. Environ. Sci.*, 2012, **5**, 9269-9290.
30. O. Shekhah, J. Liu, R. A. Fischerb, C. Woll, *Chem. Soc. Rev.*, 2011, **40**, 1081-1106.
31. X. Li, F. Cheng, S. Zhang, J. Chen, *J. Power Sources*, 2006, **160**, 542-547.
32. Q. Liu, L. Yu, Y. Wang, Y. Ji, J. Horvat, M. Cheng, X. Jia, G. Wang, *Inorg. Chem.*, 2013, **52**, 2817-2822.
33. L. Gou, L. Hao, Y. X. Shi, S. Ma, X. Fan, L. Xu, D. Li, K. Wang, *J. Solid State Chem.*, 2014, **210**, 121-124.
34. K. Saravanan, M. Nagarathinam, P. Balaya, J. J. Vittal, *J. Mater. Chem.*, 2010, **20**, 8329.
35. J. Wang, N. Yang, H. Tang, Z. Dong, Q. Jin, M. Yang, D. Kisailus, H. Zhao, Z. Tang, D. Wang, *Angew. Chem. Int. Ed.*, 2013, **52**, 6417-6420.
36. B. Liu, J. Zhang, X. Wang, G. Chen, D. Chen, C. Zhou, G. Shen, *Nano Lett.,* 2012, **12**, 3005-3011.
37. D. Ge, H. Geng, J. Wang, J. Zheng, Y. Pan, X. Cao, H. Gu, *Nanoscale*, 2014, **6**, 9689.
38. C. Li, T. Chen, W. Xu, X. Lou, L. Pan, Q. Chen, B. Hu, *J. Mater. Chem. A*, 2015, **3**, 5585-5591.
39. C. Wang, H. Wu, Z. Chen, M. T. McDowell, Y. Cui, Z. Bao, *Nat. Chem.*, 2013, **5**, 1042-1048.
40. U. Kasavajjula, C. Wang, A. J. Appleby, *J. Power Sources*, 2007, **163**, 1003-1039.
41. J. R. Szczech, S. Jin, *Energy. Environ. Sci.*, 2011, **4**, 56.
42. B. Liu, J. Zhang, X. Wang, G. Chen, D. Chen, C. Zhou, G. Shen, *Nano Lett.*, 2012, **12**, 3005-3011.
43. F. Zheng, Y. Yang, Q. Chen, Nat. Commun., 2014, **5**, 5261.

Graphical Abstract
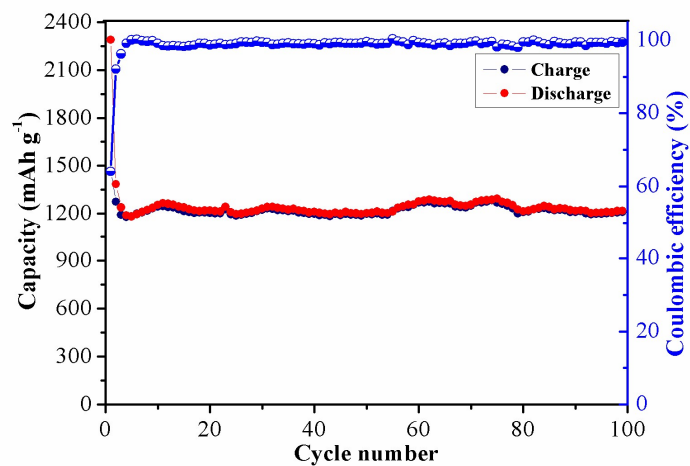
Bimetallic coordination polymers (BiCPs) with Zn and Co elements were synthesized by a simple method and applied as anode materials for the first time. When used as anode materials in LIBs, the as-prepared BiCP exhibits ultra-high capacity and impressive rate capability.